UGVA-DPNC 1998/11-180
Nov. 1998

B and D Spectroscopy at LEP

Franz Muheim*

* *Université de Genève*
Département de physique nucléaire et corpusculaire
24, quai Ernest-Ansermet, 1211 Genève 4, Switzerland
Email: Franz.Muheim@cern.ch
presented at Heavy Quarks at Fixed Target HQ98 workshop, Fermilab, Oct. 1998.

Abstract. Results from the four LEP experiments ALEPH, DELPHI, L3, and OPAL on the spectroscopy of B and charmed mesons are presented. The predictions of Heavy Quark Effective Theory (HQET) for the masses and the widths of excited $L = 1$ B mesons are supported by a new measurement from L3. A few B_c^+ candidate events have masses consistent with the recent CDF observation and the predictions. New results on D^{**} production and $B \to D^{**}\ell\nu$ are also presented. The evidence for a $D^{*'}$ meson reported recently by DELPHI is not supported by OPAL and CLEO.

INTRODUCTION

Detailed understanding of the spectroscopy of orbitally excited heavy mesons containing a b or a c quark provides important information regarding the underlying theory. A flavor-spin symmetry arises from the fact that the mass of a heavy quark Q is large relative to $\Lambda_{\rm QCD}$. In this approximation, the spin $\vec{s}_Q$ of the heavy quark Q is conserved in the interactions, independently of the total angular momentum $\vec{j}_q = \vec{s}_q + \vec{L}$ of the light quark q. Corrections to this symmetry are a series expansion in $1/m_Q, 1/m_Q^2$, calculable in Heavy Quark Effective Theory (HQET) [1].

TABLE 1. $L = 1$ B mesons containing a u or a d light quark with corresponding spin states, relative production rates, prediction for masses and widths, and two-body decay modes.

Name	j_q	J^P	**Production**	**Mass [MeV]**	**Width [MeV]**	**Decay Mode**	
B_0^*	1/2	0^+	1/12	$M_{B_1^*} - 12$	~ 150	$B\pi$	S-wave
B_1^*	1/2	1^+	3/12	$M_{B_2^*} \pm 100$	~ 150	$B^*\pi$	S-wave
B_1	3/2	1^+	3/12	5759	21	$B^*\pi$	D-wave
B_2^*	3/2	2^+	5/12	5771	25	$B^*\pi, B\pi$	D-wave

The $L = 0$ mesons, for which $j_q = 1/2$, have two possible spin states: a pseudoscalar P ($J^P = 0^-$) and a vector V ($J^P = 1^-$). If the spin of the heavy quark

is conserved independently, the relative production rate of these states is expected to be $V/(V+P) = 0.75$. Corrections due to the decay of higher excited states are predicted to be small. Recent measurements of this rate for the B system [2,3] agree well with this ratio.

In the case of $L = 1$ orbitally excited B mesons two sets of doublets are expected: the B_0^* and B_1^* ($j_q = 1/2$) and the B_1 and B_2^* ($j_q = 3/2$) mesons (see Table 1). Their relative production rate follows from spin state counting (2J+1 states) [4]. For the dominant two-body decays, the $j_q = 1/2$ states can decay via an S-wave transition and their decay widths are expected to be broad in comparison to those of the $j_q = 3/2$ states which must decay via a D-wave transition. Many measurements exist for $L = 1$ orbitally excited charm mesons. All six narrow states, a doublet (D_2^* and D_1) for each quark content ($c\bar{u}, c\bar{d}$ and $c\bar{s}$) are well established [17]. The wide $L = 1$ states are hard to measure and have not been clearly identified.

Several models based on HQET and on the charmed $L = 1$ meson data, have made predictions for the masses and widths of orbitally excited B^{**} mesons [5–9] (see Table 1). Some of these models place the average mass of the $j_q = 3/2$ states above that of the $j_q = 1/2$ states, while others predict the opposite ("spin-orbit inversion"). The mass splitting within each doublet is predicted to be 12 MeV.

B^{**} SPECTROSCOPY

At LEP excited states of B mesons are produced. Each of the four experiments has collected about 4×10^6 hadronic events out of which 0.9×10^6 events contain $B\bar{B}$ pairs. In all B^{**} analyses, first, the b-quark purity of the data sample is increased by applying a lifetime based event tag. B mesons are reconstructed inclusively. Typically the two most energetic jets of the event are considered B candidates. The decay products of the B meson are separated from the background due to fragmentation particles using secondary vertex tagging (for charged decay particles) or the rapidity of the decay products with respect to the B-jet axis. An alternative method is to fully reconstruct the B-meson decay chain which improves the resolution B-mass resolution but suffers from low statistics.

The decay of a B^{**} meson ($B^{**} \to B^{(*)}\pi$) is carried out via a strong interaction and thus the transition pion originates at the primary event vertex. In addition, the predicted masses for the $L = 1$ states correspond to relatively small Q values, so that the pion direction is forward with respect to the B-meson direction. The track with the largest component of momentum in the direction of the B jet is selected.

A first measurement of $L = 1$ orbitally excited B mesons has been presented by OPAL [10]. Using secondary vertex charge tagging to inclusively reconstruct B mesons, the invariant mass distributions of $B^{(*)+}\pi^-$ and $B^{(*)+}K^-$ combinations show enhancements consistent with the decay of B^{**} resonances as shown in Fig. 1. An excess of 1738 ± 121 $B^{(*)+}\pi^-$ and 149 ± 30 $B^{(*)+}K^-$ candidates is observed in the mass ranges 5.60 - 5.85 GeV and 5.80 - 6.00 GeV, respectively. The background

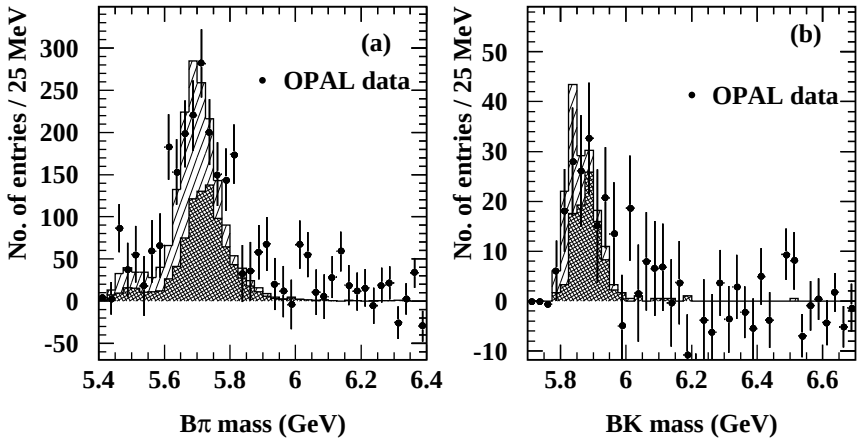

FIGURE 1. The invariant mass distribution for (a) $B^{(*)+}\pi^-$ and (b) $B^{(*)+}K^-$ combinations after subtraction of the background, respectively. The solid histograms shows the contribution from the B_2^* and the hatched histogram shows the contribution from the B_1 state.

is estimated with the wrong (like)-sign combinations. Fitting the excess with a single Breit-Wigner function yields an average mass $M(B^{**}_{u,d})$ and a production rate $f_{B^{**}} = \mathcal{B}(b \to B^{**}_{u,d})/\mathcal{B}(b \to B_{u,d})$. Throughout this paper, isospin symmetry is always employed to account for B^{**} decays via neutral pions. DELPHI and ALEPH have made similar measurements using rapidity to inclusively reconstruct B mesons [11,12]. The results are summarized in Table 2.

TABLE 2. Inclusive B^{**} measurements.

	$M(B^{**}_{u,d})$ [MeV]	$f_{B^{**}}$
OPAL	5681 ± 11	0.270 ± 0.056
DELPHI	$5734 \pm 5 \pm 17$	$0.32 \pm 0.018 \pm 0.06$
ALEPH	$5703 \pm 4 \pm 10$	$0.279 \pm 0.016 \pm 0.059\ ^{+0.039}_{-0.056}$

A new measurement using an exclusive method is presented by ALEPH [13]. Using many decay modes ($B \to D^{(*)}X$, where $X \in [\pi, \rho, a_1]$ and $B \to J/\psi(\psi')K^{(*)}$) 238 charged and 166 neutral B meson candidates have been fully reconstructed. The sample has a B meson purity of 85 %. Each B candidate is then combined with a charged pion from the primary vertex. An excess of 45 ± 13 events is seen in the right-sign sample compared to the wrong-sign sample. Fig. 2 shows a fit to the right-sign mass spectrum where the signal shape consists of five Breit-Wigner peaks. The relative masses, the widths, and the relative production rates of the individual B^{**} mesons have been fixed to the predictions from HQET. The mass of

the B_2^* meson and the overall production rate are measured to be:

$$M_{B_2^*} = 5739\ ^{+8}_{-11}\ ^{+6}_{-4}\ \text{MeV}$$
$$f_{B^{**}} = 0.31 \pm 0.09\ ^{+0.06}_{-0.05} \quad .$$

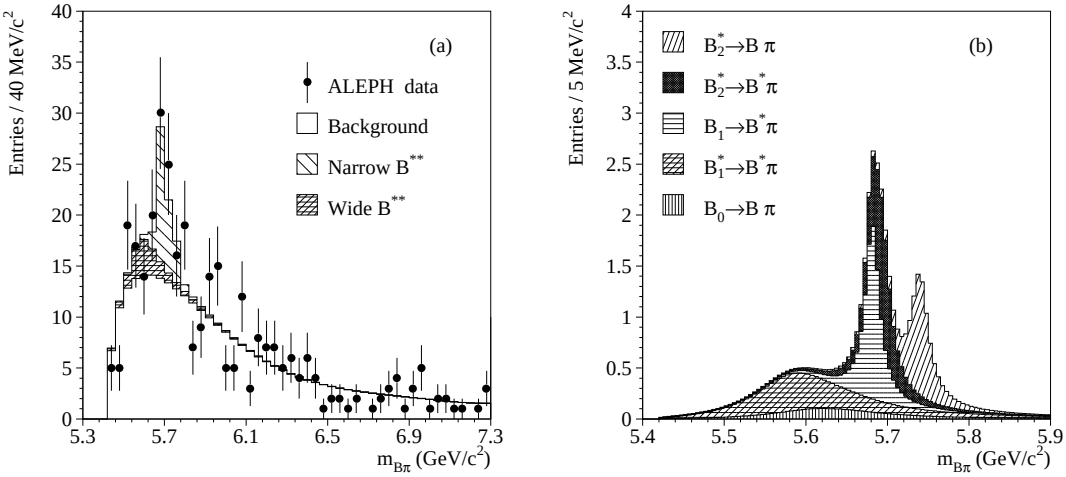

FIGURE 2. (a) Bπ mass spectrum from data. The fit (histogram) includes the expected background plus contributions from the narrow and wide B** states. (b) An expanded view of the signal region.

A new analysis using an inclusive method is presented here by the L3 experiment [14]. Several techniques are used to both improve on the resolution of the Bπ mass spectrum and to unfold this resolution from the signal components. As a result, L3 is able to extract measurements for the masses and widths of both the D-wave B_2^* decays and the S-wave B_1^* decays.

B meson candidates are reconstructed inclusively from all charged and neutral particles with rapidity $y > 1.6$ relative to the original jet axis. The measurement of the direction of the B meson is determined by an error-weighted average of the direction of the measured secondary decay vertex and of the direction of the B candidate. The angular resolution obtained is $\sigma_1 = 12$ mrad for ϕ, and $\sigma_1 = 18$ mrad for θ, respectively. The energy of the B meson candidate, E_B, is estimated by taking advantage of the known center-of-mass energy at LEP, E_{cm}, to be

$$E_B = \frac{E_{cm}^2 - M_B^2 + M_{recoil}^2}{2E_{cm}} \quad , \tag{1}$$

where M_{recoil} is the mass of all particles in the event recoiling against the B candidate. The difference between reconstructed and generated values for the B-meson energy can be described by an asymmetric Gaussian with widths of 1.9 GeV and 2.8 GeV.

Fig. 3a) shows the resulting $B\pi$ invariant mass spectrum together with the expected background from Monte Carlo. A clear signal due $B^{**} \to B^{(*)}\pi$ decays is seen above the background which is well described by the simulation. Thus the background is parameterized by a threshold function, the shape of which is determined from the Monte Carlo.

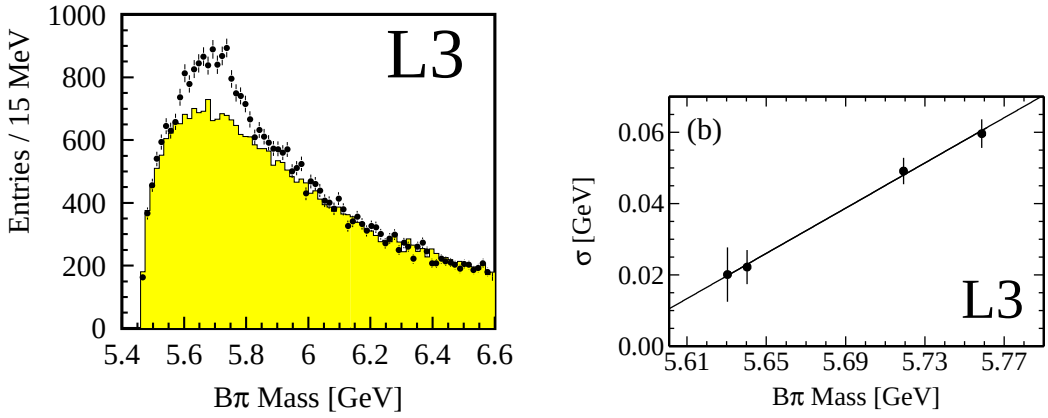

FIGURE 3. (a) Mass spectrum for selected $B\pi$ pairs. The dots are data and the shaded histogram represents the expected background from Monte Carlo normalized to the sideband region $6.0 - 6.6$ GeV. (b) Linear fit to the extracted $B\pi$ mass resolution for Monte Carlo signal components generated at four different B^{**} mass values.

To resolve the underlying structure of the signal, it is necessary to unfold effects due to detector resolution. The dominant sources of uncertainty for the mass measurement are, with about equal magnitude, the angular and energy resolution of the B meson. The dependence of the $B\pi$ mass resolution on the B^{**} mass is studied by simulating signal events at four different values of B^{**} mass and Breit-Wigner width. Each signal $B\pi$ mass distribution is then fit to a Breit-Wigner function convoluted with a Gaussian resolution. The Breit-Wigner width is fixed to its generated value and the Gaussian resolution is extracted from the fit and shown in Fig. 3b) as a function of the $B\pi$ mass together with a linear parameterization. The mass resolution is increasing with increasing $B\pi$ mass.

The fit function for the signal consists of five Breit-Wigner mass peaks one for the each of the five decay modes allowed by spin-parity rules: $B_2^* \to B\pi, B^*\pi$, $B_1 \to B^*\pi$, $B_1^* \to B^*\pi$, and $B_0^* \to B\pi$. Each Breit-Wigner width is convoluted with the mass dependent Gaussian resolution. No attempt is made to tag subsequent $B^* \to B\gamma$ decays, as the efficiency for selecting the soft photon is low. The relative production rate, and the mass splittings and the relative width within each doublet are constrained to the predictions from HQET (see Table 1).

The $B\pi$ invariant mass distribution fit with the signal and background function described above is shown in Fig. 4. The results of the fit provide the first mea-

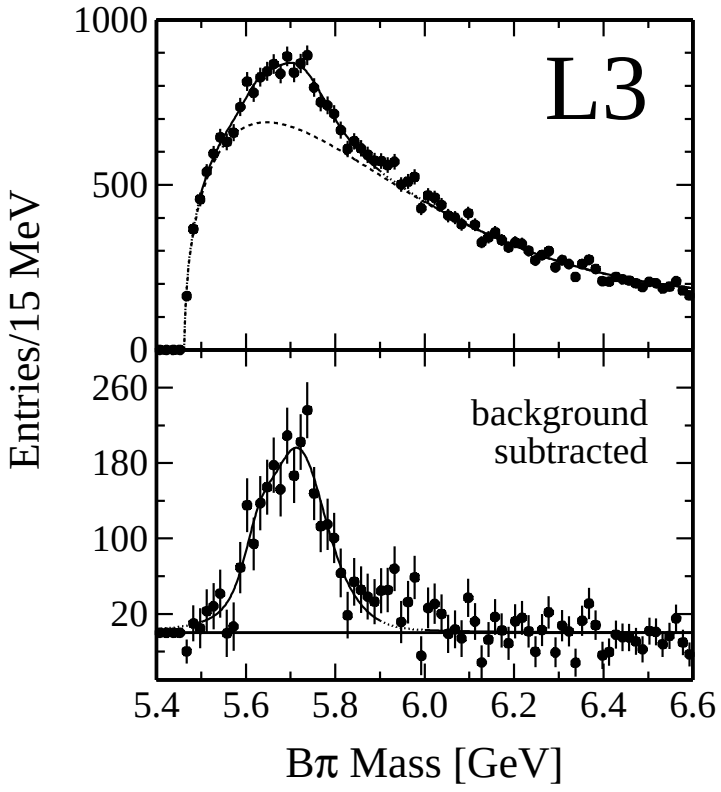

FIGURE 4. Fit to the data Bπ mass distribution with the five-peak signal function and the background function described in the text.

surements of the masses and decay widths of the B_2^* ($j_q = 3/2$) and B_1^* ($j_q = 1/2$) mesons:

$$\begin{aligned} M_{\mathrm{B}_2^*} &= (5770 \pm 6\ (\mathrm{stat.}) \pm 4(\mathrm{syst}))\ \ \mathrm{MeV} \\ \Gamma_{\mathrm{B}_2^*} &= (21 \pm 24\ (\mathrm{stat.}) \pm 15(\mathrm{syst}))\ \ \mathrm{MeV} \\ M_{\mathrm{B}_1^*} &= (5675 \pm 12\ (\mathrm{stat.}) \pm 4(\mathrm{syst}))\ \ \mathrm{MeV} \\ \Gamma_{\mathrm{B}_1^*} &= (75 \pm 28\ (\mathrm{stat.}) \pm 15(\mathrm{syst}))\ \ \mathrm{MeV} \quad . \end{aligned}$$

A total of 2652 ± 232 events that occupy the signal region correspond to a relative production rate $f_{\mathrm{B}^{**}}$ for all $L = 1$ spin states of

$$f_{\mathrm{B}^{**}} = 0.39 \pm 0.06\ (\mathrm{stat.}) \pm 0.06(\mathrm{syst}) \quad .$$

Systematic errors are mainly due to the modelling of the background, the limited knowledge of the signal function and the mass constraint within the doublets.

These results disfavor recent theoretical models proposing spin-orbit inversion [8,9], but do agree well with several earlier models [5–7] and provide strong support for HQET.

B_c^+ STUDIES

DELPHI, ALEPH, and OPAL have published searches for B_c^+ mesons in Z decays [15]. No signals have been found. Table 3 shows the number of candidate events and the obtained upper limits on the production rates $\mathcal{B}(Z \to B_c^+ X) \times \mathcal{B}(B_c^+ \to J/\psi\pi^+, J/\psi\ell^+\nu, J/\psi\pi^+\pi^-\pi^+)$. The 3 $B_c^+ \to J/\psi\pi^+$ candidates are consistent with

TABLE 3. B_c^+ studies at LEP.

Decay mode	**Candidates**			**Prod. Limit** $[10^{-5}]$ **at 90% CL**		
	DELPHI	ALEPH	OPAL	DELPHI	ALEPH	OPAL
$B_c^+ \to J/\psi\pi^+$	1	0	2	10.5 to 8.4	3.6	10.6
$B_c^+ \to J/\psi\ell^+\nu$	0	2	1	5.8 to 5.0	5.2	6.96
$B_c^+ \to J/\psi\pi^+\pi^-\pi^+$	1	-	0	17.5	-	5.53

a background estimate of 2.3 expected events. A fit to the mass yields the following values: $M_{J/\psi\pi^+} = 6.342 \pm 0.027$ GeV (DELPHI) and $M_{J/\psi\pi^+} = 6.32 \pm 0.06$ GeV (OPAL average), respectively. Predictions for the B_c^+ mass are in the range 6.24 to 6.31 GeV. The CDF experiment at the Tevatron has recently reported the observation of the B_c^+ meson in the decay channel $B_c^+ \to J/\psi\ell^+\nu$ [16]. They find $20.4\ ^{+6.2}_{-5.8}$ events and obtain a mass value of $M(B_c^+) = 6.40 \pm 0.39 \pm 0.13$ GeV.

D^{**} SPECTROSCOPY

During the last year several new results on D^{**} production have been presented by the LEP collaborations. D^{**0} mesons are fully reconstructed in the decay chain

TABLE 4. D^{**} production fractions $\mathcal{B}$ [%].

Production mode	**OPAL**	**DELPHI**	**ALEPH**
$b \to {D_1}^0$	$5.0 \pm 1.4 \pm 0.6$	2.0 ± 0.6	2.3 ± 0.7
$b \to D_2^{*0}$	$4.7 \pm 2.4 \pm 1.3$	4.8 ± 2.0	< 2.0
$c \to {D_1}^0$	$2.1 \pm 0.7 \pm 0.3$	1.9 ± 0.4	1.6 ± 0.5
$c \to D_2^{*0}$	$5.2 \pm 2.2 \pm 1.3$	4.7 ± 1.3	4.7 ± 1.0
$c \to D_{s1}^+$	$1.6 \pm 0.4 \pm 0.3$	-	$0.77 \pm 0.20 \pm 0.08$
$c \to D_{s2}^{*+}$	-	-	$1.3 \pm 0.5 \pm 0.2$
$b \to D_{s1}^+$	-	-	$1.1 \pm 0.3 \pm 0.2$
$b \to D_{s2}^{*+}$	-	-	$2.2 \pm 0.8 \pm 0.5$

$D^{**0} \to D^{*+}\pi^-$, $D^{*+} \to D^0\pi^+$, $D^0 \to K^-\pi^+$. High momentum D^{**0} together with short decay lengths are selected to obtain $c\bar{c}$ enriched samples whereas B and D meson vertexing is used to select $b\bar{b}$ enriched samples. Table 4 shows the results for the D^{**} production fractions measured by OPAL, DELPHI, and ALEPH [18–20].

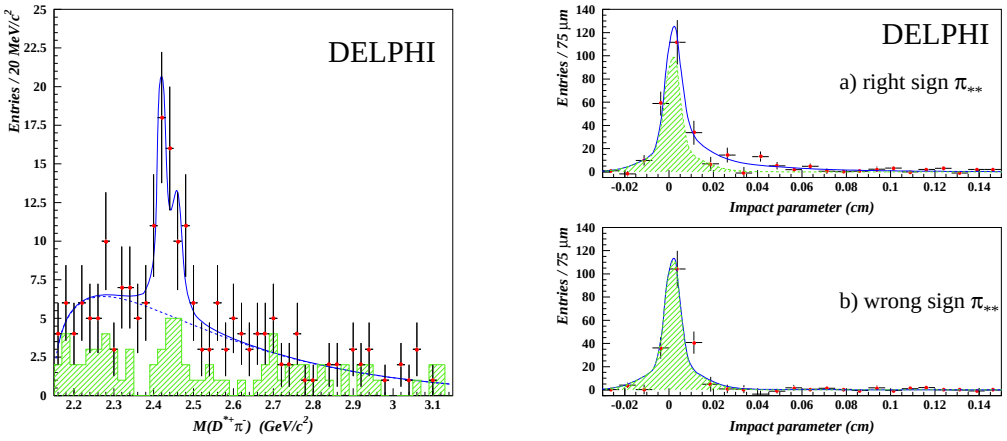

FIGURE 5. (a) Experimental $D^{*+}\pi^-$ invariant mass distribution for $D^{*+}\pi^-\ell^-$ events. The solid line is a fit to the narrow D^{**} states plus background. The wrong sign $D^{*+}\pi^-\ell^+$ candidates are shown in the hatched histogram. (b) Impact parameter relative to the primary event vertex for right charge and wrong charge π_{**} candidates. The fit is described in the text.

DELPHI has also presented a new $B \to D^{**}\ell\nu$ analysis [21]. In semileptonic events, the decay chain $D^{*+} \to D^0\pi^+$, $D^0 \to K^-\pi^+, K^-\pi^+\pi^-\pi^+, K^-\pi^+(\pi^0)$ is fully reconstructed. The D^{*+} candidates are then combined with opposite sign π^- and the $D^{*+}\pi^-$ mass, shown in Fig. 5a), is fit to the narrow D^{**} states, resulting in the following branching fraction: $\mathcal{B}(B^- \to D_1{}^0\ell^-\bar{\nu}) = 0.72 \pm 0.22 \pm 0.13\%$.

A fit to the impact parameter distribution of the bachelor pion π_{**} stemming from the $D^{**} \to D^*\pi$ transition for right (unlike)-sign and wrong (like)-sign combinations, as shown in Fig. 5b), allows to extract the following branching fraction $\mathcal{B}(B^- \to D^{*+}\pi^-\ell^-\bar{\nu}) = 1.15 \pm 0.17 \pm 0.14\%$ where the signal comprises narrow and wide D^{**} resonances plus non-resonant $D^{*+}\pi^-$ combinations. These results are in agreement with previous LEP and CLEO measurements.

$D^{*\prime}$ STUDIES

DELPHI has recently reported an excess of events in the $D^{*+}\pi^-\pi^+$ mass spectrum as shown in Fig. 6a) [22]. The fit yields $N = 66 \pm 14$ events, corresponding to a production rate $f_{D^{*\prime}}/f_{D^{**}} = 0.49 \pm 0.18 \pm 0.10$, a mass $M = 2637 \pm 2 \pm 6$ MeV and a width consistent with the experimental resolution. This mass value is consistent with predictions of a radial excited $D^{*\prime}$ meson.

OPAL has performed a similar analysis [23]. The resulting $D^{*+}\pi^-\pi^+$ mass spectrum is shown in Fig. 6b) for data and Monte Carlo events, where a DELPHI-like signal has been added in the simulation. No excess is seen in the data ($N < 32.8$ at 95 % CL) corresponding to a limit on the production rate of $f_{D^{*\prime}}/f_{D^{**}} < 0.21$ at 95 % CL, thus not confirming the DELPHI result. CLEO also has examined their $D^{*+}\pi^-\pi^+$ mass spectrum and does not confirm the DELPHI evidence [24].

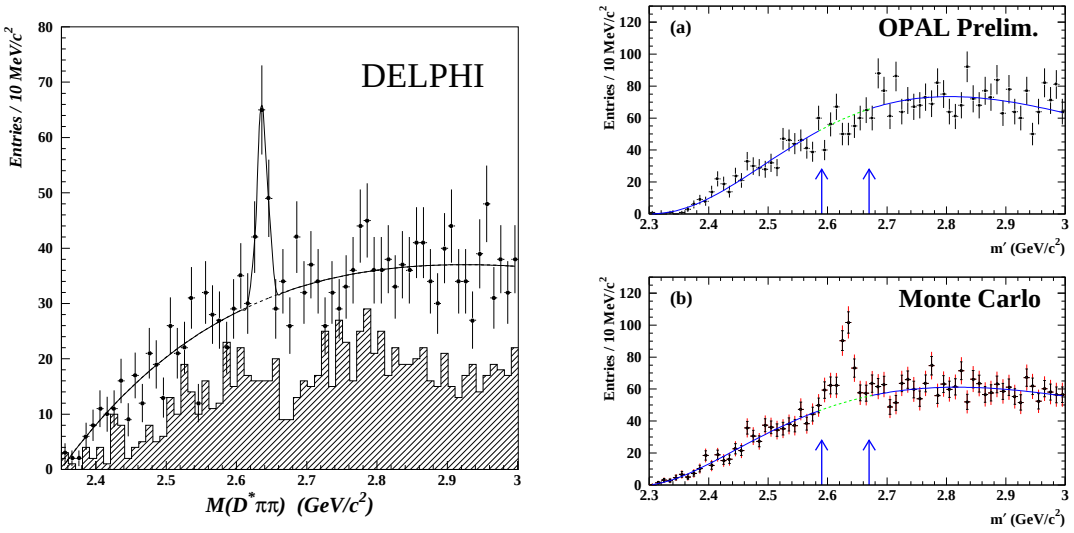

FIGURE 6. (a) DELPHI invariant mass distributions $D^{*+}\pi^+\pi^-$ (dots) and $D^{*+}\pi^-\pi^-$ (hatched histogram). (b) OPAL $D^{*+}\pi^+\pi^-$ mass distribution for data and Monte Carlo. A DELPHI-like signal has been added in the simulation.

ACKNOWLEDGEMENTS

I wish to thank my colleagues from the other LEP collaborations for providing me with the results and the figure files. I also thank S. Goldfarb for his help when preparing this presentation.

REFERENCES

1. N. Isgur and M.B. Wise, Phys. Lett. **B 232** (1989) 113; Phys. Lett. **B 237** (1990) 527; Their overview "Heavy Quark Symmetry" is included in *B Decays*, revised 2nd edition, edited by S. Stone (World Scientific, 1994) 231 and in *Heavy Flavors*, edited by A.J. Buras and M. Lindner (World Scientific, 1992) 234.
2. L3 Collaboration, Phys. Lett. **B 345** (1995) 589; Contribution to EPS Conference, Brussels EPS95 (1995).

3. DELPHI Collaboration, Z. Phys. **C 68** (1995) 353;
ALEPH Collaboration, Z. Phys. **C 69** (1996) 393;
OPAL Collaboration, Z. Phys. **C 74** (1997) 413.
4. J.L. Rosner, Comments Nucl. Part. Phys. **16** (1986) 109;
N. Isgur and M.B. Wise, Phys. Rev. Lett. **66** (1991) 1130.
5. M. Gronau, A. Nippe and J.L. Rosner, Phys. Rev. **D 47** (1993) 1988;
M. Gronau and J.L. Rosner, Phys. Rev. **D 49** (1994) 254.
6. E.J. Eichten, C.T. Hill and C. Quigg, Phys. Rev. Lett. **71** (1993) 4116; Fermilab-Conf-94/118-T (1994).
7. A.F. Falk and T. Mehen, Phys. Rev. **D 53** (1996) 231.
8. N. Isgur, Phys. Rev. **D 57** (1998) 4041.
9. D. Ebert, V.O. Galkin and R.N. Faustov, Phys. Rev. **D 57** (1998) 5663.
10. OPAL Collaboration, Z. Phys. **C 66** (1995) 19.
11. DELPHI Collaboration, Phys. Lett. **B 345** (1995) 598; Contribution to EPS conference, Brussels EPS95 (1995).
12. ALEPH Collaboration, Z. Phys. **C 69** (1996) 393.
13. ALEPH Collaboration, Phys. Lett. **B 425** (1998) 215.
14. L3 Collaboration, to be submitted to Phys. Lett. **B**.
15. DELPHI Collaboration, Phys. Lett.**B 398** (1997) 207;
ALEPH Collaboration, Phys. Lett.**B 402** (1997) 213;
OPAL Collaboration, Phys. Lett.**B 420** (1998) 157.
16. CDF Collaboration, Phys. Rev. Lett. **81**(1998) 2432; Phys. Rev. **D 58**(1998) 112004.
17. ARGUS Collaboration, Phys. Rev. Lett. **56** (1986) 549; Phys. Lett. **B 221** (1989) 422; Phys. Lett. **B 231** (1989) 208; Z. Phys. **C 69** (1996) 405;
CLEO Collaboration, Phys. Rev. **D 41** (1990) 774; Phys. Lett. **B 303** (1993) 377; Phys. Lett. **B 331** (1994) 236; Phys. Lett. **B 340** (1994) 194; Phys. Rev. Lett. **72** (1994) 1972;
E691 Collaboration, Phys. Rev. Lett. **62** (1989) 1717;
E687 Collaboration, Phys. Rev. Lett. **72** (1994) 324;
BEBC Collaboration, Z. Phys. **C 61** (1994) 563;
ALEPH Collaboration, Phys. Lett. **B 345** (1994) 103; Z. Phys. **C 62** (1994) 1; Z. Phys. **C 73** (1997) 601.
18. OPAL Collaboration, Z. Phys. **C 76** (1997) 425.
19. DELPHI Collaboration, Contribution to ICHEP98 conference, Vancouver, (1998), paper # 240.
20. ALEPH Collaboration, Contribution to ICHEP98 conference, Vancouver, (1998), papers # 943 and # 944.
21. DELPHI Collaboration, Contribution to ICHEP98 conference, Vancouver, (1998), paper #239.
22. DELPHI Collaboration, Phys. Lett. **B 426** (1998) 231.
23. OPAL Collaboration, Contribution to ICHEP98 conference, Vancouver, (1998), paper # 1037
24. CLEO Collaboration, Contribution to ICHEP98 conference, Vancouver, (1998).